



Hydride, alkyl and carbyne derivatives of the unsaturated heterometallic anion $[\text{MoWCp}_2(\mu\text{-PCy}_2)(\mu\text{-CO})_2]^-$

M. Angeles Alvarez, M. Esther García, Daniel García-Vivó*, Estefanía Huergo, Miguel A. Ruiz**

Departamento de Química Orgánica e Inorgánica/IUQOEM, Universidad de Oviedo, E-33071, Oviedo, Spain

ARTICLE INFO

Article history:

Received 8 March 2019

Received in revised form

24 April 2019

Accepted 26 April 2019

Available online 30 April 2019

Keywords:

Heterometallic complexes

Metal–metal interactions

Carbonylate complexes

Hydride complexes

Carbyne complexes

Agostic complexes

ABSTRACT

The heterometallic hydride $[\text{MoWCp}_2(\mu\text{-H})(\mu\text{-PCy}_2)(\text{CO})_4]$ was prepared in 30% yield through reaction of an equimolar mixture of $[\text{Mo}_2\text{Cp}_2(\text{CO})_6]$ and $[\text{W}_2\text{Cp}_2(\text{CO})_6]$ with a two-fold excess of PHCy_2 in xylene solution, in a sealed tube at 453 K. The sodium salt of the title anion was then prepared from the latter hydride in a three-step process first involving dehydrogenation with $\text{HBF}_4 \cdot \text{OEt}_2$ in dichloromethane to give the cationic derivative $[\text{MoWCp}_2(\mu\text{-PCy}_2)(\text{CO})_4](\text{BF}_4)$, then reaction of the latter with NaI in refluxing 1,2-dichloroethane to yield the iodide-bridged dicarbonyl complex $[\text{MoWCp}_2(\mu\text{-I})(\mu\text{-PCy}_2)(\text{CO})_2]$ and, finally, reaction of the latter with $\text{Na}(\text{Hg})$ in tetrahydrofuran solution. Reaction of this anion with $(\text{NH}_4)\text{PF}_6$ gave the hydride $[\text{MoWCp}_2(\text{H})(\mu\text{-PCy}_2)(\text{CO})_2]$, which in solution displays an equilibrium mixture of two isomers, one with terminal carbonyls and the hydride ligand bridging the metal atoms (**B**), another one with a semibridging carbonyl and the hydride ligand terminally bound to the W atom (**T**). The prevalence of isomer **T** was higher than the observed ones in the corresponding homometallic analogues, and there was a clear thermodynamic preference of the hydride ligand for the W site, estimated in some 20 kJ/mol according to density functional theory (DFT) calculations. The title anion reacted selectively with benzyl chloride at room temperature, to give the agostic benzyl-bridged derivative $[\text{MoWCp}_2(\mu\text{-}\kappa^1\text{:}\eta^2\text{-CH}_2\text{Ph})(\mu\text{-PCy}_2)(\text{CO})_2]$, which displays specific κ^1 -coordination to the W atom ($\text{Mo}-\text{W} = 2.580(1)$ Å), while the analogous reaction with MeI gave a mixture of the related methyl-bridged complex $[\text{MoWCp}_2(\mu\text{-}\kappa^1\text{:}\eta^2\text{-CH}_3)(\mu\text{-PCy}_2)(\text{CO})_2]$ and its methoxycarbyne-bridged isomer $[\text{MoWCp}_2(\mu\text{-COMe})(\mu\text{-PCy}_2)(\mu\text{-CO})]$ in a ratio of ca. 5:1, with the latter corresponding to a chemical behaviour intermediate between those of its homonuclear analogues. Photolysis of the above alkyl complexes with visible-UV light at room temperature resulted in fast decarbonylation followed by dehydrogenation, to give the corresponding carbyne-bridged derivatives $[\text{MoWCp}_2(\mu\text{-CR})(\mu\text{-PCy}_2)(\mu\text{-CO})]$ ($\text{R} = \text{H}, \text{Ph}$) in good yield. This suggests that the cooperative action of Mo and W atoms greatly reduces the thermal barrier of the C–H bond cleavage steps required for dehydrogenation of the alkyl ligands in these substrates.

© 2019 Elsevier B.V. All rights reserved.

1. Introduction

Mononuclear transition-metal carbonylates are classical reagents in organometallic chemistry. Due to their good nucleophilic properties, these anionic metal complexes react under mild conditions with a large variety of electrophilic molecules, whereby new bonds can be made between the metal atom and virtually any

other element in the periodic table [1]. Even after many decades of extensive research, however, interesting new findings are just appearing in the field, as novel anions with unusual structures, electron counts, or metal atoms are being unveiled [2]. Compared to this state of facts, the chemistry of binuclear carbonylates has been much less developed, due to the scarce number of species available for reactivity studies. This is particularly so in the case of binuclear anions bearing metal-metal multiple bonds, of which only a few examples are known, and even fewer of them can be properly used in synthetic studies, these being essentially limited to the 32-electron complexes $[\text{Mn}_2(\text{CO})_6(\mu\text{-Ph}_2\text{PCH}_2\text{PPh}_2)]^{2-}$ [3], and $[\text{Fe}_2(\mu\text{-PPh}_2)(\text{CO})_6]^-$ [4], with $\text{M} = \text{M}$ bonds, and to the 30-electron complexes $[\text{M}_2\text{Cp}_2(\mu\text{-PR}_2)(\mu\text{-CO})_2]^-$ ($\text{M} = \text{Mo}, \text{R} = \text{Cy}$ [5],

* Corresponding author.

** Corresponding author.

E-mail addresses: garciavdaniel@uniovi.es (D. García-Vivó), mar@uniovi.es (M.A. Ruiz).

^tBu [6]; M = W, R = Cy [7]), which display M≡M bonds. Extensive studies carried out in our lab on the latter dicarbonyl anions have shown that the combined presence of negative charge and an intermetallic multiple bond confers a wide synthetic potential to these complexes, this enabling the synthesis of a great variety of derivatives with many different functionalities including, *inter alia*, bridging hydride, alkyl, alkenyl and carbyne ligands. Such synthetic versatility in turn derives from the activity of two distinct nucleophilic sites in these anions, located at the dimetal site and oxygen atoms of the bridging carbonyls, respectively [8].

The above studies have also revealed a significant influence of the metal (Mo vs. W) on the reactivity of these unsaturated anions, which is well exemplified by the protonation and methylation reactions of the PCy₂-bridged anions (Scheme 1). Thus, while protonation of the Mo₂ anion with (NH₄)PF₆ gives a hydride-bridged product, the W₂ anion renders an equilibrium mixture of two isomers, which bear either bridging or terminal hydride ligands, respectively (**B** and **T** in Scheme 1) [7b,9–11]. On the other hand, while reaction of the Mo₂ anion with MeI results in electrophile attachment at the dimetal site to yield an agostic methyl-bridged derivative, the analogous reaction of the W₂ anion gives a mixture of the related methyl complex (minor product) and the methoxycarbyne-bridged isomer following from electrophile attachment at the oxygen atom of a bridging carbonyl (major product), this proving the higher nucleophilicity of the O-site at the ditungsten anion [7a].

Having realized the significant influence of the metal on the chemistry of these anions, we then undertook a search for related unsaturated anions containing Mo≡W bonds, so to examine the effects that the presence of such intermetallic multiple bond would have on the reactivity of these anionic species, such as site selectivity and cooperative effects, and also on the structure of their neutral derivatives. We note that, although there is currently a substantial research activity around coordination compounds bearing heterometallic multiple bonds [12], there are only few studies concerning related organometallic compounds [13,14]. Of particular relevance in the context of 30-electron complexes is the

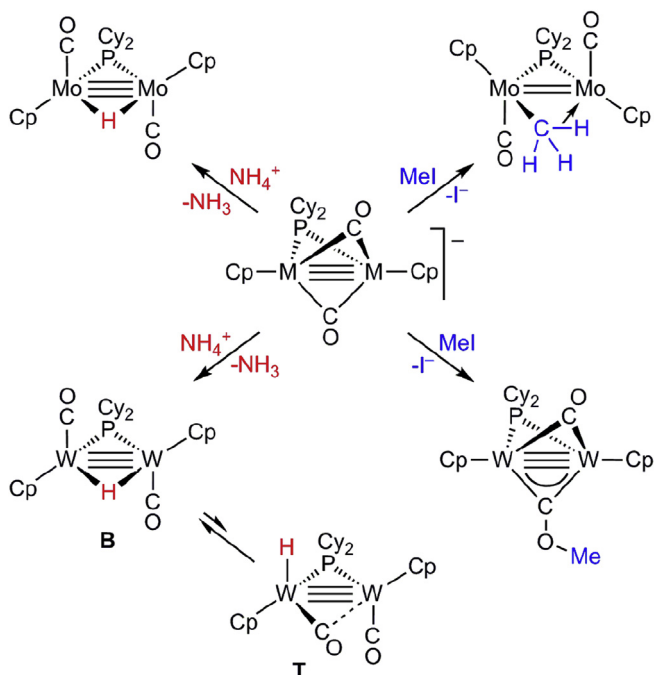
finding by Suzuki et al. that the unsaturated hydride [Cp*₃Ru(μ-H)₄OsCp*] undergoes addition reactions at a rate much higher than the rates measured for the corresponding homometallic complexes having Ru–Ru or Os–Os bonds, thus proving the operation of a true cooperative kinetic effect in this heterometallic system [14d]. In this paper we report an efficient preparative route to the 30-electron heterometallic anion [MoWCp₂(μ-PCy₂)(μ-CO)₂][−], which is the first reported carbonyl anion with a heterometallic triple bond, and a study on the formation and structure of some of their neutral derivatives bearing hydride, alkyl or carbyne ligands. As will be shown below, these studies prove the operation of definite structural effects (coordination preferences), and also suggest that the cooperative action of Mo and W greatly reduces the thermal barrier of the C–H bond cleavage steps required for dehydrogenation of alkyl ligands at these heterometallic centres.

2. Results and discussion

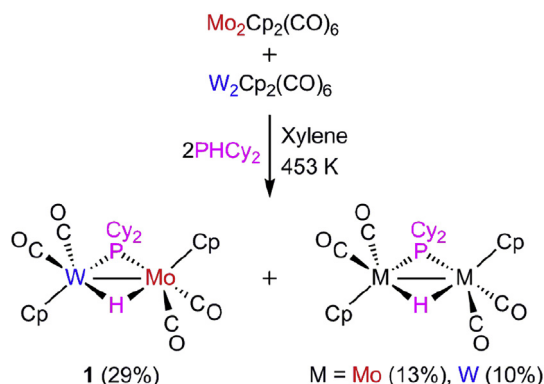
2.1. Synthesis of the heterometallic hydride precursor **1**

The formation of homometallic anions [M₂Cp₂(μ-PCy₂)(μ-CO)₂][−] (M = Mo, W) ultimately relies on the reduction of the corresponding halide-bridged complexes [M₂Cp₂(μ-X)(μ-PCy₂)(CO)₂], which in turn can be prepared either through direct reaction of [M₂Cp₂(CO)₆] with chlorophosphine PCy₂Cl, when M = Mo [5], or *via* a two-step reaction starting from the electron-precise hydride [M₂Cp₂(μ-H)(μ-PCy₂)(CO)₄], when M = W [7]. The latter proved to be the only successful route to our targeted halide-bridged intermediate [MoWCp₂(μ-X)(μ-PCy₂)(CO)₂], but this in turn required implementing an efficient preparation for the corresponding heterometallic precursor, the new hydride complex [MoWCp₂(μ-H)(μ-PCy₂)(CO)₄] (**1**). Attempts to prepare compound **1** through the routes used previously to synthesize related homometallic complexes [M₂Cp₂(μ-H)(μ-PRR')(CO)₄] (reactions of [M₂Cp₂(CO)₆] or [M₂Cp₂(CO)₄] with HPRR', or reaction of [M₂Cp₂(CO)₄] with LiPRR') [15,16] proved to be inefficient in this case. Eventually, compound **1** could be efficiently prepared through a slight modification of the method reported by Haupt et al. to obtain related MoRe hydride complexes [17]. Thus, the reaction of an equimolar mixture of [Mo₂Cp₂(CO)₆] and [W₂Cp₂(CO)₆] with a two-fold excess of PHCy₂ in xylene solution, in a sealed tube at 453 K for 6 h, rendered an almost statistical mixture of the hydride-bridged complexes [MM'Cp₂(μ-H)(μ-PCy₂)(CO)₄] (Scheme 2), from which the heterometallic complex **1** could be eventually isolated in ca. 30% yield after chromatographic workup.

Spectroscopic data in solution for compound **1** (Table 1 and Experimental section) are comparable to those of the



Scheme 1. Reactivity of unsaturated homometallic anions.



Scheme 2. Synthesis of the heterometallic compound **1**.

Table 1
Selected IR and NMR data for new compounds.

Compound	$\nu(\text{CO})^a$	$\delta(\text{P}) [J_{\text{PW}}]^b$	$\delta(\mu\text{-C}) [J_{\text{CP}}]^b$
[MoWCp ₂ ($\mu\text{-H}$)($\mu\text{-PCy}_2$)(CO) ₄] (1)		1922 (vs), 1847 (s)	178.9 [197] ^c
[MoWCp ₂ ($\mu\text{-PCy}_2$)(CO) ₄](BF ₄) (2)		2003 (m), 1961 (vs), 1934 (s), 1907 (m, sh)	170.1 [255]
[MoWCp ₂ ($\mu\text{-I}$)($\mu\text{-PCy}_2$)(CO) ₂] (3)		1866 (m, sh), 1829 (vs)	125.8 [307] ^c
Na[MoWCp ₂ ($\mu\text{-PCy}_2$)($\mu\text{-CO}$) ₂] (4-Na)		1565 (vs) ^d	
[MoWCp ₂ ($\mu\text{-H}$)($\mu\text{-PCy}_2$)(CO) ₂] (5B)		1869 (w, sh), 1821 (vs)	197.3 [330] ^e
[MoWCp ₂ (H)($\mu\text{-PCy}_2$)(CO) ₂] (5T)		1762 (s) ^f	232.8 [248] ^e
[MoWCp ₂ ($\mu\text{-}\kappa^1\text{-}\eta^2\text{-CH}_3$)($\mu\text{-PCy}_2$)(CO) ₂] (6)		1854 (m, sh), 1812 (vs)	116.5 [310]
[MoWCp ₂ ($\mu\text{-COMe}$)($\mu\text{-PCy}_2$)($\mu\text{-CO}$)] (7)		1653 (vs)	194.5 [345]
[MoWCp ₂ ($\mu\text{-}\kappa^1\text{-}\eta^2\text{-CH}_2\text{Ph}$)($\mu\text{-PCy}_2$)(CO) ₂] (8)		1865 (m, sh), 1823 (vs)	111.2 [305]
[MoWCp ₂ ($\mu\text{-CH}$)($\mu\text{-PCy}_2$)($\mu\text{-CO}$)] (9)		1661 (vs)	195.0 [345]
[MoWCp ₂ ($\mu\text{-CPh}$)($\mu\text{-PCy}_2$)($\mu\text{-CO}$)] (10)		1662 (vs)	199.7 [341]
[MoWCp ₂ ($\mu\text{-PCy}_2$) ₂ ($\mu\text{-CO}$)] (11)		1638 (vs)	203.6 [364] ^c

^a Recorded in dichloromethane solution, data in cm⁻¹.

^b Recorded at room temperature in CD₂Cl₂ solution at 162.01 (³¹P) and 100.63 MHz (¹³C), unless otherwise stated; δ in ppm relative to external 85% aqueous H₃PO₄ and internal tetramethylsilane, respectively, with ³¹P–¹⁸³W and ¹³C–³¹P coupling constants (J_{PW} and J_{CP}) in Hz.

^c Recorded in C₆D₆.

^d Recorded in tetrahydrofuran solution.

^e Recorded at 162.01 MHz and 183 K.

^f Another C–O stretch is obscured by the 1821 cm⁻¹ band of isomer **5B** (see text).

^g Recorded at 183 K.

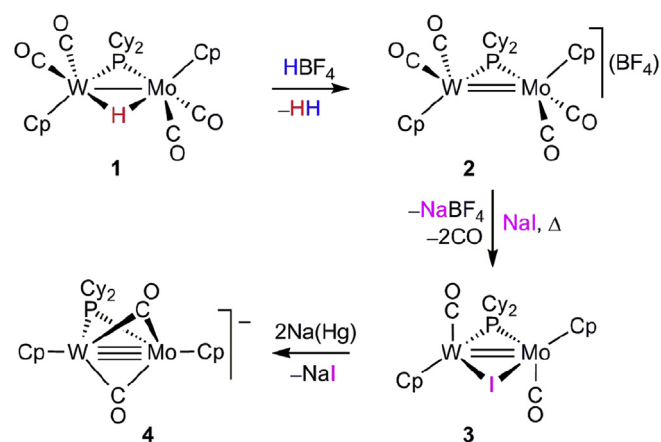
^h Recorded at 233 K.

corresponding Mo₂ and W₂ analogues and related complexes [15,16], and need not to be discussed in detail. All these molecules display a transoid arrangement of their MCp(CO)₂ fragments, which has been substantiated through X-ray studies in several cases [16,18]. As expected, compound **1** displays ³¹P (δ_{P} 178.9 ppm) and hydride (δ_{H} –14.56 ppm, J_{HP} = 30 Hz) resonances in positions intermediate with respect to its homometallic analogues, with one-bond P–W (197 Hz) and H–W (40 Hz) couplings comparable to those measured in the corresponding ditungsten complex (182 and 40 Hz, respectively). As for the carbonyl ligands of **1**, the presence of Mo and W atoms in the same molecule removes all symmetry elements, so all of them become inequivalent, with the ones positioned *cis* to the P atom rendering ¹³C NMR resonances displaying measurable two-bond P–C couplings of ca. 20–30 Hz as expected [19,20].

2.2. Synthesis and structural characterization of the title anion and its heterometallic precursors

As noted above, the title anion could be efficiently prepared using the synthetic route previously developed for the related ditungsten analogue [7], a three-step process starting from the corresponding 34-electron hydride [M₂Cp₂($\mu\text{-H}$)($\mu\text{-PCy}_2$)(CO)₄] (Scheme 3). In the first step, the heterometallic hydride **1** is dehydrogenated through reaction with HBF₄·OEt₂ in dichloromethane solution, to yield the 32-electron cationic derivative [MoWCp₂($\mu\text{-PCy}_2$)(CO)₄](BF₄) (**2**). Spectroscopic data for **2** (Table 1 and Experimental section) are comparable to those of its ditungsten analogue [7] and related PPh₂-bridged complexes [21]. In particular, we note the significant increase in the C–O stretches (relative to **1**) as a result of the presence of a positive charge in the complex, while the increased one-bond P–W coupling (from 197 to 255 Hz) reflects the reduction in the number of ligands surrounding the W atom after dehydrogenation [20].

In the second step, the cationic complex **2** is reacted with an excess NaI in refluxing 1,2-dichloroethane solution, whereby iodide addition and decarbonylation takes place, to yield the iodide-bridged dicarbonyl complex [MoWCp₂($\mu\text{-I}$)($\mu\text{-PCy}_2$)(CO)₂] (**3**) almost quantitatively. As found for its ditungsten analogue, this 32-



Scheme 3. Synthesis of the unsaturated heterometallic anion **4**.

electron complex is quite air-sensitive and was used without further purification. Its IR spectrum displays two C–O stretching bands with relative intensities (weak and strong, in order of decreasing frequencies) characteristic of transoid M₂(CO)₂ oscillators [22]. This structural arrangement has been persistently found in all halide-bridged complexes of type [M₂Cp₂($\mu\text{-X}$)($\mu\text{-PR}_2$)(CO)₂] prepared by us previously, and it has been substantiated crystallographically in the case of [Mo₂Cp₂($\mu\text{-Cl}$)($\mu\text{-P}^t\text{Bu}_2$)(CO)₂] [6]. The ³¹P NMR resonance of **3** is substantially shielded with respect to **1** (125.8 vs. 178.9 ppm), as usually found in this family of neutral complexes, and the one-bond P–W coupling is substantially higher (307 vs. 197 Hz), thus reflecting the significant reduction in the coordination number around the W atom after decarbonylation.

In the last step, the iodide-bridged complex **3** is reduced with Na(Hg) in tetrahydrofuran solution, whereby the sodium salt of the targeted unsaturated anion Na[MoWCp₂($\mu\text{-PCy}_2$)($\mu\text{-CO}$)₂] (**4-Na**) is formed in a quantitative way, along with NaI. This product is very air-sensitive and displays low solubility in tetrahydrofuran, thus precluding its analysis by NMR spectroscopy. Its IR spectrum displays a single and strong C–O stretch at very low frequency

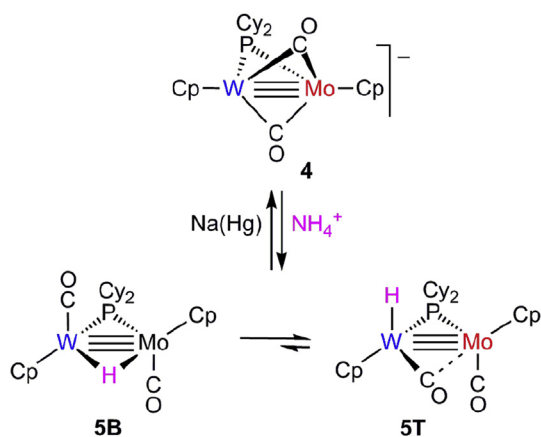
(1565 cm^{-1}), in a position intermediate with respect to those measured for the analogous Mo_2 and W_2 complexes (1580 and 1546 cm^{-1} , respectively), which corresponds to the asymmetric stretch for the $\text{M}_2(\mu\text{-CO})_2$ oscillator of these anions. The expected and weaker band corresponding to the symmetric stretch probably is too close to the latter band, to be observed separately.

We have shown previously that strong ion-pairing effects are present in the solutions of these unsaturated anions, which are in turn strongly dependent on their counter-ion [5a]; this is also the case for the heterometallic anion **4**. For instance, the lithium salt $\text{Li}[\text{MoWCp}_2(\mu\text{-PCy}_2)(\mu\text{-CO})_2]$ (**4-Li**) could be analogously prepared by reacting **3** with $\text{Li}(\text{Hg})$ in tetrahydrofuran solution. Interestingly, as found for its Mo_2 analogue, the IR spectrum of this salt now displays three C–O stretches at 1642 (w), 1573 (m, sh) and 1552 (s) cm^{-1} , with the latter two bands likely corresponding respectively to the symmetric and asymmetric stretches of the isolated anion (with unspecific cation–anion interactions), while the band at 1642 cm^{-1} can be attributed to the C–O stretch of a tight ion pair involving the attachment of the Li^+ cation to one of the bridging carbonyls [5a].

2.3. Formation and structural characterization of the hydride complex **5**

The sodium salt of anion **4** reacts readily with the weak acid $(\text{NH}_4)\text{PF}_6$ in tetrahydrofuran solution to give the corresponding hydride $[\text{MoWCp}_2(\text{H})(\mu\text{-PCy}_2)(\text{CO})_2]$ (**5**), which can be isolated in good yield as a pure substance upon chromatographic workup. Protonation of **4** with strong acids such as $\text{HBF}_4 \cdot \text{OEt}_2$ led only to complex mixtures of unstable products. We note, however, that the protonation process leading to **5** is fully reversible, since **4-Na** can be selectively regenerated upon stirring a tetrahydrofuran solution of **5** with $\text{Na}(\text{Hg})$ for a few minutes.

Complex **5** exists in solution as an equilibrium mixture of two isomers, one with terminal carbonyls and the hydride ligand bridging the metal atoms (**5B**), another one with a semibridging carbonyl and the hydride ligand terminally bound to the W atom (**5T**) (Scheme 4), as previously found for its ditungsten analogue (Scheme 1). These structural types have been characterized crystallographically for the dimolybdenum complexes $[\text{Mo}_2\text{Cp}_2(\mu\text{-H})(\mu\text{-PCy}_2)(\text{CO})_2]$ (isomer **B**) [23], and $[\text{Mo}_2\text{Cp}_2(\text{H})(\mu\text{-P}^t\text{Bu}_2)(\text{CO})_2]$ (isomer **T**) [6]; the latter complexes, however, displayed in solution a single isomer in each case. In the case of **5**, the isomer ratio **T/B** expectedly was solvent- and temperature-dependent but, interestingly, has a value outside the range spanned by its homometallic analogues (**T/B** ca. 0 and 0.33 in CD_2Cl_2 solution at 193 K



respectively for the Mo_2 and W_2 analogues), since under analogous conditions the terminal isomer **5T** is the major species in solution (**5T/5B** = 2.5 at 183 K). This can be then considered as a genuine heterometallic effect of structural nature. Isomer **5T** was also found to be favoured over isomer **5B** on lowering the temperature, but disfavoured when using a less polar solvent as toluene- d_8 (**5T/5B** = 0.6 at 183 K) (see the Experimental section). In any case, all of this means that the energetic difference between these two isomers in **5** is very small, in agreement with density functional theory (DFT) calculations [24] discussed below.

Spectroscopic data for isomers **5B** and **5T** are comparable to those of their homometallic analogues where applicable, and need not to be discussed in detail. The presence of the terminal isomer **5T** at room temperature is denoted by the appearance of a C–O stretch at 1762 cm^{-1} in the IR spectrum, indicative of the presence of a semibridging carbonyl ligand, in addition to the more energetic bands at 1869 (w, sh) and 1821 (vs) cm^{-1} expected for the stretches of antiparallel terminal carbonyls in the hydride-bridged isomer **5B**. Separate NMR resonances could be observed for both isomers at low temperature (see the Experimental section), with the terminal isomer **5T** reproducing the spectroscopic features of its ditungsten analogue: (a) a ^{31}P NMR resonance more deshielded than isomer **5B** (δ_{P} 232.8 vs. 197.3 ppm); (b) a lower one-bond P–W coupling (248 vs. 330 Hz), as expected from the higher coordination number at the W atom; (c) a less shielded hydride resonance (δ_{H} –1.46 vs. –6.41 ppm), indicative of its terminal coordination, with a high H–W coupling of 70 Hz which denotes its attachment specifically at the W site (cf. δ –0.71 ppm, J_{HW} = 99 Hz for its W_2 analogue); and (d) a strong deshielding of the W-bound carbonyl (δ_{C} 276.2 ppm) indicative of its semibridging character (cf. 272.7 ppm in its W_2 analogue). All these data provide conclusive evidence for a clear preference of the hydride ligand in **5** for terminal coordination specifically at the W site, a matter further analysed below.

2.3.1. DFT calculations on hydride **5**

To gain more insight concerning the structures and relative stability of different isomers of compound **5** in solution we have performed DFT calculations on the observed isomers **5B** and **5T**, and also on a third isomer similar to the latter one, but with the hydride ligand terminally bound to the Mo atom, and the Mo-bound carbonyl involved in semibridging interaction with the W atom (**5T-Mo**) (Fig. 1 and Table 2, see the Experimental section and

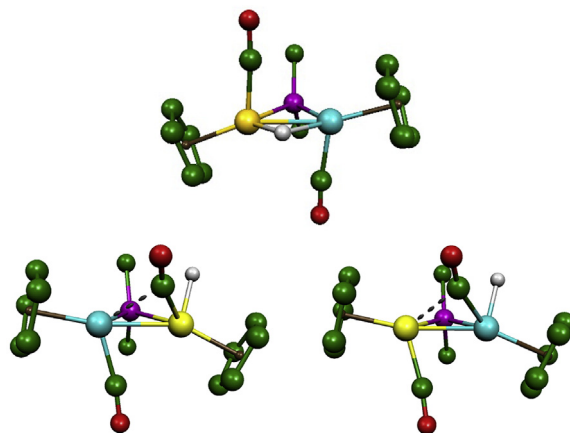


Fig. 1. B3LYP-optimized structures for isomers **5B** (upper, blue colour for Mo), **5T** (lower, left) and **5T-Mo** (lower, right), with H atoms (except hydride ligands) and Cy groups (except C^1 atoms) omitted for clarity. Relative Gibbs free energies at 295 K were 0, +11 and +31 kJ/mol respectively. (For interpretation of the references to colour in this figure legend, the reader is referred to the Web version of this article.)

Table 2
B3LYP-computed bond lengths (Å) and angles (°) for different isomers of compound **5**.

parameter	5B	5T	5T-Mo
W–Mo	2.544	2.536	2.531
W–P	2.427	2.452	2.395
Mo–P	2.449	2.413	2.476
W–CO	1.950	1.982	1.945
W···CO		2.775	2.395
Mo–CO	1.953	1.951	1.990
Mo···CO		2.442	2.761
W–H	1.851	1.707	
Mo–H	1.895		1.692
W–C–O	175.5	166.1	172.4
Mo–C–O	173.9	171.1	162.6
W–Mo–CO	81.3	74.5	62.6
Mo–W–CO	84.3	64.1	74.9

Supplementary data). The latter isomer displays a structure essentially equivalent to that of **5T**, but was computed to be some 20 kJ/mol less stable than **5T** in the gas phase, which is consistent with the experimental fact that no significant amounts of such isomer are detected spectroscopically in solution, and with the general finding that W–H bonds are generally stronger than Mo–H bonds in comparable organometallic species [25]. Therefore we can conclude that the observed preference of the hydride ligand for terminal coordination at the W (instead of Mo) site is of thermodynamic origin.

Concerning the geometries computed for the observed isomers **5B** and **5T**, we notice that the structural parameters for these molecules at the B3LYP level are in good agreement with those determined crystallographically for the dimolybdenum hydrides $[\text{Mo}_2\text{Cp}_2(\mu\text{-H})(\mu\text{-PCy}_2)(\text{CO})_2]$ and $[\text{Mo}_2\text{Cp}_2(\text{H})(\mu\text{-P}^t\text{Bu}_2)(\text{CO})_2]$ respectively [6,22], although the computed distances involving the metal atoms are slightly higher than the experimental values in the Mo_2 complexes, as commonly found at this level of calculation [24]. These structures in turn are comparable to those computed at the same level for isomers of type **B** and **T** for the above P^tBu_2 -bridged complex, or for the ditungsten analogue of **5**, which we have analysed previously in detail [7b,9]. Then, only a few comments are to be added: (a) The intermetallic separation in isomers **5B** and **5T** (ca. 2.54 Å) is very short and similar to each other, in line with our general view that the triply bonding intermetallic interaction in this sort of complex is not significantly modified by the coordination mode (bridging or terminal) of the hydride ligand [11b]; (b) The carbonyl bound to the metal atom bearing the terminal hydride (W) is involved in a significant semibringing interaction with the other metal atom (Mo), as denoted by the Mo···CO length of 2.442 Å, in agreement with the ^{13}C NMR data discussed above, while the W–C–O angle remains high (166.1°), this enabling its classification as linear semibringing of type II [26], which is a common structural feature of compounds displaying intermetallic triple bonds; the Mo-bound carbonyl displays a much longer separation to the W atom (W···CO 2.775 Å) and then must be considered as essentially terminal.

Our calculations at the B3LYP level predict that the hydride-bridged isomer **5B** is more stable (by 11 kJ/mol) than the terminal isomer **5T** in the gas phase, which is consistent with the experimental fact that **5B** is the major species in toluene- d_8 solution at 183 K. Dispersion forces seem to be of no critical role on the relative stability of these isomers, as inclusion of the Grimme correction in our calculations (see the Experimental section) only reduced from 11 to 9.5 kJ/mol the energy difference between isomers. However, as noted above, isomer **5T** is the major species in dichloromethane solution at all temperatures. Inclusion of solvation effects (see the

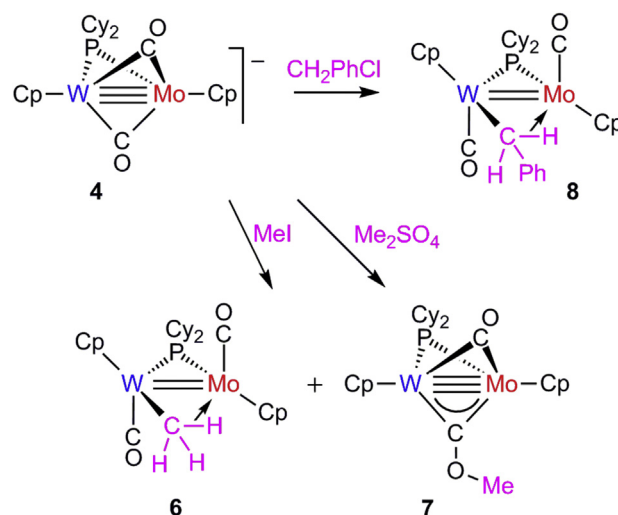
Experimental section) only marginally reduced the energetic difference between these isomers (to ca. 8 kJ/mol), but still did not reproduce the experimental prevalence of **5T** in such solvent. This might suggest that interactions between the terminal isomer **5T** and the dichloromethane molecules might be more specific than conventional dipole-dipole interactions, perhaps being of hydrogen-bond nature. Interestingly, hydrogen-bond interactions between the hydride complex $[\text{WCp}(\text{CO})_3\text{H}]$ and dichloromethane molecules have been computed to be of significant strength (ca 9 kJ/mol) [27], enough to influence in our case the thermodynamic balance between isomers **5B** and **5T** in solution.

2.4. Reactions of anion **4** with alkyl halides

The sodium salt of anion **4** reacts slowly with excess MeI at room temperature in tetrahydrofuran solution, to give a mixture of the methyl-bridged complex $[\text{MoWCp}_2(\mu\text{-}\kappa^1\text{:}\eta^2\text{-CH}_3)(\mu\text{-PCy}_2)(\text{CO})_2]$ (**6**) and its methoxycarbonyl-bridged isomer $[\text{MoWCp}_2(\mu\text{-COMe})(\mu\text{-PCy}_2)(\mu\text{-CO})]$ (**7**), in a ratio of ca. 5:1 (Scheme 5). This corresponds to a chemical behaviour intermediate between those of its homometallic analogues, which in the same reaction instead yielded only the methyl derivative (Mo_2) or mostly the methoxycarbonyl isomer (W_2), as noted above (Scheme 1). Expectedly, the carbonyl complex **7** could be selectively prepared by using a stronger methylating reagent [5a], in this case methyl sulfate (see the Experimental section). In contrast, **Na-4** reacts selectively with benzyl chloride under the same conditions, to give the benzyl-bridged derivative $[\text{MoWCp}_2(\mu\text{-}\kappa^1\text{:}\eta^2\text{-CH}_2\text{Ph})(\mu\text{-PCy}_2)(\text{CO})_2]$ (**8**) as the sole product, as found for the Mo_2 and W_2 related anions.

2.4.1. Solid-state and solution structure of the agostic benzyl-bridged complex **8**

The molecule of **8** in the crystal (Fig. 2 and Table 3) is built from two transoid $\text{MCp}(\text{CO})$ fragments bridged by a PCy_2 group and an agostic methyl ligand which is κ^1 -bound to the tungsten atom (W–C = 2.26(2) Å) and η^2 -bound to the Mo atom via a C–H bond (Mo–C = 2.40(2), Mo–H = 2.00(2) Å), whereby it formally contributes with three electrons to the dimetal site, which in turn leads to the proposal for **8** of an intermetallic double bond, according to the 18-electron rule. This is consistent with the intermetallic separation of 2.580(1) Å in **8**, which is ca. 0.06 Å longer than the corresponding length of 2.528(2) Å in the 30-electron hydride $[\text{Mo}_2\text{Cp}_2(\mu\text{-H})(\mu\text{-PCy}_2)(\text{CO})_2]$ [23], although still some 0.08 Å



Scheme 5. Alkylation reactions of anion **4**.

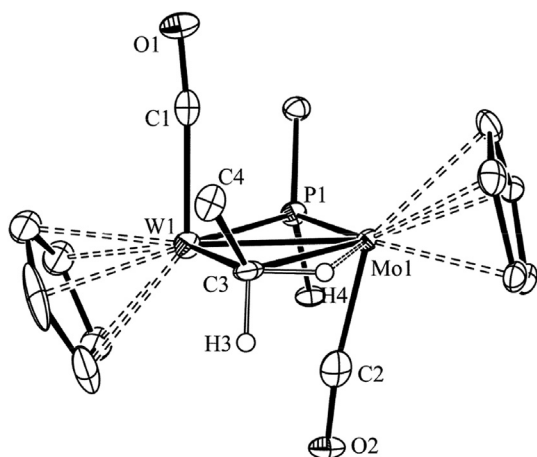


Fig. 2. ORTEP diagram (30% probability) of compound **8**, with Ph and Cy groups (except their C¹ atoms) and most H atoms omitted for clarity.

Table 3
Selected bond lengths (Å) and angles (°) for **8**.

W(1)–Mo(1)	2.580(1)	W(1)–P(1)–Mo(1)	65.4(1)
W(1)–P(1)	2.380(4)	W(1)–C(3)–Mo(1)	67.2(5)
Mo(1)–P(1)	2.394(4)	Mo(1)–W(1)–C(1)	86.7(4)
W(1)–C(1)	1.96(2)	W(1)–Mo(1)–C(2)	73.8(5)
Mo(1)–C(2)	1.93(2)	P(1)–W(1)–C(1)	85.4(5)
W(1)–C(3)	2.26(2)	P(1)–Mo(1)–C(2)	81.9(5)
Mo(1)–C(3)	2.40(2)	P(1)–W(1)–C(3)	116.5(4)
C(3)–H(4)	1.03(2)	P(1)–Mo(1)–C(3)	110.9(4)
Mo(1)–H(4)	2.00(2)	C(1)–W(1)–C(3)	90.0(6)
		C(2)–Mo(1)–C(3)	81.0(7)

shorter than the figure expected for a double bond (cf. 2.666(1) Å in the 32-electron complex [Mo₂Cp₂(μ-CPh)(μ-PCy₂)(CO)₂] [28]. All of these structural parameters actually are very similar to those measured for the related homometallic complex [Mo₂Cp₂(μ-κ¹:η²-CH₂Ph)(μ-PCy₂)(CO)₂] (Mo–Mo = 2.580(1) Å), a molecule for which the strength of the η²-bonding interaction of the benzyl ligand has been estimated to be 89 kJ/mol, according to DFT calculations [29].

Spectroscopic data in solution for **8** (Table 1 and Experimental section) are consistent with the structure found in the crystal, and also are comparable to those measured for its Mo₂ and W₂ analogues [29,7a], so a detailed discussion is not needed. The retention in solution of the agostic coordination of the benzyl ligand in **8** is first indicated by the corresponding ³¹P NMR data (δ_p 112.2 ppm, J_{PW} = 305 Hz), which are comparable to those of the iodide-bridged complex **3**, thus suggesting an effective three-electron contribution of the methyl ligand to the dimetal site. In addition, the involvement of one of the C–H bonds in a tricentric interaction with a metal atom is denoted by the strong shielding of one of the methylenic ¹H resonances, which appears at –2.02 ppm (cf. –1.35 ppm and –2.50 ppm respectively for the corresponding Mo₂ and W₂ analogues).

2.4.2. Solution structure of the agostic methyl complex **6**

Spectroscopic IR and ³¹P NMR data in solution for **6** (Table 1 and Experimental section) are similar to those of **8**, thus suggesting that both compounds are isostructural. In the case of **6**, however, there is no direct evidence for the agostic coordination of the methyl ligand, as the three H atoms remained equivalent on the NMR time scale at all temperatures, giving rise to a single resonance at ca. –0.87 ppm which remained unchanged down to 183 K. The same observations were made previously for the corresponding homometallic

analogues (δ_H = –0.77 and –1.18 ppm respectively for the Mo₂ and W₂ complexes) [29,7a], and they seem to be derived from the operation in all cases of a fast dynamic process involving the chemical exchange of all H atoms of the methyl ligand [29]. Actually, the averaged C–H coupling of 122 Hz for **6** is somewhat lower than the corresponding value in the Mo₂ complex [124 Hz], which might indicate a C–H···Mo interaction a bit stronger for the heterometallic complex.

To obtain further support for the agostic coordination of the methyl ligand in **6** and its selective κ¹-coordination to the tungsten atom (as found for the benzyl complex **8**), we carried out DFT calculations on this molecule. We first note that, although models with κ¹-coordination to either Mo or W were attempted, only the latter rendered a minimum on the corresponding potential energy surface (Fig. 3), with geometrical parameters comparable to those experimentally determined for the benzyl complex **8**. Therefore we conclude that there is a clear site preference of the alkyl ligands in these κ¹:η²-bridged complexes, which favours κ¹-coordination specifically to the W atom, in line with the higher strength of W–C bonds (when compared to Mo–C ones) usually found in organometallic complexes [25b,30].

We also wondered whether an isomer bearing a terminal methyl ligand (that is, analogous to the terminal hydride isomer **5T**) might be a sensible structure in this heterometallic system. Indeed we found that such a structure (**6T-W**, Fig. 3) is a true minimum with geometrical parameters comparable to those of **5T**, including a comparably short intermetallic length of 2.54 Å consistent with the formulation of an intermetallic triple bond, as required on application of the 18-electron rule, and the presence of a linear semi-bridging carbonyl. The Gibbs free energy for **6T-W** in the gas phase was only some 10 kJ/mol higher than that of **6T**, so we cannot exclude its presence in the solutions of compound **6**, even if in tiny amounts. As for the agostic isomer **6**, the intermetallic length is expectedly longer (2.594 Å) and comparable to the experimental value measured in the benzyl complex **8** (2.580(1) Å), because the η² coordination of the C–H bond now provides additional electron density to the dimetal site, in detriment of the intermetallic interaction [29].

2.5. Dehydrogenation of the agostic alkyl complexes **6** and **8**

We have shown previously that photolysis of the benzyl-bridged homometallic complexes [M₂Cp₂(μ-κ¹:η²-CH₂Ph)(μ-PCy₂)(CO)₂] (M = Mo, W) results in decarbonylation and dehydrogenation of the benzyl group, to give the corresponding benzyldiyne-bridged derivatives [28,7a]. In contrast, photolysis of the related methyl-

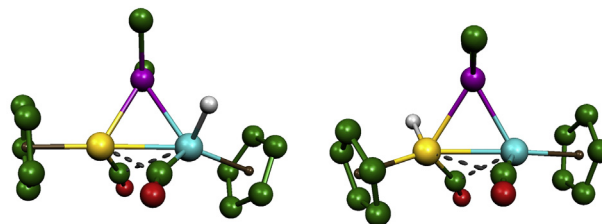
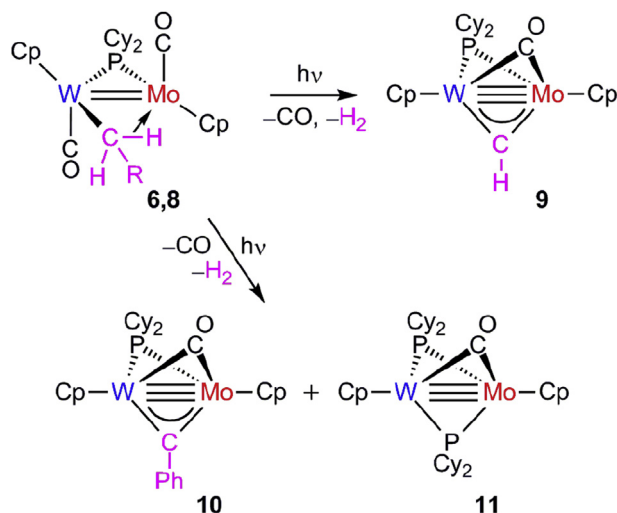


Fig. 3. B3LYP-optimized structures for compound **6** (left) and an isomer having a terminal Me group bound to the W (yellow) atom (**6T-W**, right), with most H atoms and Cy groups (except C¹ atoms) omitted for clarity. Relative Gibbs free energies at 295 K were 0 and + 10 kJ/mol respectively. Selected bond lengths for **6** (Å): Mo–W = 2.594; W–CH₃ = 2.282; Mo–CH₃ = 2.465; Mo···H = 2.206; C–H···Mo = 1.114; Mo–P = 2.448; W–P = 2.428. Selected bond lengths for **6T-W**: Mo–W = 2.540; W–CH₃ = 2.240; W–CO = 1.979; Mo···CO = 2.398; H₂C–H (average) = 1.096; Mo–P = 2.424; W–P = 2.485. (For interpretation of the references to colour in this figure legend, the reader is referred to the Web version of this article.)

bridged complex $[\text{Mo}_2\text{Cp}_2(\mu-\kappa^1:\eta^2\text{-CH}_3)(\mu\text{-PCy}_2)(\text{CO})_2]$ only resulted in decarbonylation of the dimetal substrate, to yield the 30-electron methyl-bridged derivative $[\text{Mo}_2\text{Cp}_2(\mu-\kappa^1:\eta^2\text{-CH}_3)(\mu\text{-PCy}_2)(\mu\text{-CO})]$ [31]. Recently, however, we found that the presence of the bulkier P^tBu_2 group in these substrates somehow facilitates the dehydrogenation of bridging methyl ligands, so that the related complex $[\text{Mo}_2\text{Cp}_2(\mu-\kappa^1:\eta^2\text{-CH}_3)(\mu\text{-P}^t\text{Bu}_2)(\mu\text{-CO})]$ could be transformed easily into the corresponding methylidyne-bridged derivative upon gentle heating at 353 K [6]. It was thus of interest to examine the influence of the heterometallic MoW site on the dehydrogenation processes of the alkyl ligands present in complexes **6** and **8**.

Irradiation of toluene solutions of **6** with visible-UV light at 288 K resulted in decarbonylation and dehydrogenation to give the corresponding methylidyne-bridged complex $[\text{MoWCp}_2(\mu\text{-CH})(\mu\text{-PCy}_2)(\mu\text{-CO})]$ (**9**) as major product (Scheme 6), along with small amounts of compound **1**, the latter obviously arising from some competing decomposition pathway. Since our previous studies on dehydrogenation reactions of the P^tBu_2 -bridged alkyl complexes revealed that the C–H cleavage steps leading to dehydrogenation are thermal processes following photochemical decarbonylation [6], then the formation of **9** at room temperature suggests that the cooperative action of Mo and W atoms in these substrates greatly reduces the thermal barrier of the C–H bond cleavage steps required for dehydrogenation of the methyl ligand. Unfortunately, we have no information concerning the photochemistry of the ditungsten complex $[\text{W}_2\text{Cp}_2(\mu-\kappa^1:\eta^2\text{-CH}_3)(\mu\text{-PCy}_2)(\text{CO})_2]$ [7a], so more conclusive evidence for heterometallic effects in these dehydrogenation processes is not possible at this stage.

According to the mentioned studies on Mo_2 substrates, the thermal barrier for the C–H bond cleavage steps leading to dehydrogenation are lower for the agostic benzyl ligands, when compared to the methyl ligands. Thus it was not surprising to find that photolysis of toluene solutions of the benzyl complex **8** at 288 K also resulted in easy dehydrogenation to yield the corresponding benzylidyne-bridged derivative $[\text{MoWCp}_2(\mu\text{-CPh})(\mu\text{-PCy}_2)(\mu\text{-CO})]$ (**10**). In this case, however, small amounts of the bis(phosphanide) complex $[\text{MoWCp}_2(\mu\text{-PCy}_2)_2(\mu\text{-CO})]$ (**11**) were formed as a side product (Scheme 6). The latter was identified by comparison of its IR and ^{31}P NMR data (Table 1) with those of related homometallic analogues $[\text{M}_2\text{Cp}_2(\mu\text{-PR}_2)_2(\mu\text{-CO})]$ ($\text{M} = \text{Mo}, \text{W}; \text{R} = \text{Cy}, \text{Ph}$) [15,32], and no attempts to fully characterize it were made.



Scheme 6. Photolysis of agostic alkyl complexes.

2.5.1. Structural characterization of carbyne-bridged complexes **7**, **9** and **10**

Spectroscopic data for the carbyne-bridged complexes **7**, **9** and **10** are comparable to each other and also to those of related homometallic Mo_2 and W_2 complexes [5–7,28], then requiring no detailed discussion. We note that this family of 30-electron complexes has been structurally characterized in several cases [8], whereby very short intermetallic lengths of ca. 2.47 Å have been found in all cases. This is consistent with the triple bond to be proposed for these molecules on the basis of the 18-electron rule, more precisely described as following from a $\sigma^2\delta^4$ configuration, according to DFT calculations [33].

All these molecules are built from MCp fragments bridged by three different ligands: phosphanide, carbonyl and carbyne. The former gives rise to a strongly deshielded ^{31}P NMR resonance at ca. 195 ppm, characteristic of 30-electron complexes, which also displays high one-bond P–W couplings of ca. 345 Hz denoting the low coordination number of the tungsten atom in these molecules. The carbyne ligand gives rise to diagnostic strongly deshielded ^{13}C NMR resonances (ca. 350–375 ppm), while the methylidyne ligand in **9** also accounts for a highly deshielded ^1H NMR resonance at 18.70 ppm (cf. 16.74 ppm for its crystallographically characterized Mo_2 analogue) [28]. The bridging carbonyl ligand in these complexes gives rise to a ^{13}C resonance at ca. 300 ppm as expected, and the corresponding C–O stretch for compounds **9** and **10** is observed at ca. 1661 cm^{-1} , a frequency which is reduced by some 10 cm^{-1} in the methoxycarbyne complex **7** ($\nu_{\text{CO}} = 1653 \text{ cm}^{-1}$), a difference which can be attributed to the increased electron density at the dimetal site resulting from the π -bonding interaction present in the C–O bond of alkoxy-carbyne ligands [33].

3. Conclusions

As found for its homometallic analogues, the heterometallic anion **4** displays multisite reactivity, with nucleophilic sites located at the dimetal centre and the O atoms of the bridging carbonyls, as the reaction with MeI illustrates. In this respect, anion **4** displays a chemical behaviour intermediate between those observed for the Mo_2 and W_2 analogues. The hydride derivative of **4** displays two isomers in solution, as found for the W_2 system, yet two additional structural effects can be appreciated in the heterometallic system: (a) a clear thermodynamic preference of the hydride ligand for terminal coordination at the W site (vs. Mo), estimated in some 20 kJ/mol according to DFT calculations; and (b) a clear prevalence of the terminal isomer (**T**) vs. the hydride-bridged one (**B**), when compared to either of the Mo_2 or W_2 homometallic systems, which can be then considered as a genuine heterometallic effect. A defined structural preference is also observed for the agostic methyl and benzyl derivatives of **4**, which specifically are κ^1 -bound to the W atom, while one of the C–H bonds binds the Mo atom. The methyl ligand in the heterometallic complex is dehydrogenated much more easily than their Mo_2 analogues, which suggests another genuine heterometallic effect, i.e. that the cooperative action of Mo and W atoms in these substrates greatly reduces the thermal barrier of the C–H bond cleavage steps required for such dehydrogenation.

4. Experimental

All reactions and manipulations were carried out under a nitrogen atmosphere using standard Schlenk techniques. Solvents were purified according to literature procedures [34], and distilled under nitrogen prior to use. Petroleum ether refers to that fraction distilling in the range 338–343 K, and the xylene used actually was a mixture of the corresponding *o*- *m*- and *p*-isomers. Complex

$[W_2Cp_2(CO)_6]$ ($Cp = \eta^5-C_5H_5$) was prepared as described previously [35]. All other reagents were obtained from the usual commercial suppliers and used as received. Photochemical experiments were performed using jacketed Schlenk tubes, cooled by tap water (ca. 288 K). A 400 W mercury lamp placed ca. 1 cm away from the Schlenk tube was used for all experiments. Chromatographic separations were carried out using jacketed columns refrigerated by tap water (ca. 288 K) or by a closed 2-propanol circuit kept at the desired temperature with a cryostat. Commercial aluminium oxide (activity I, 70–290 mesh) was degassed under vacuum prior to use. The latter was mixed under nitrogen with the appropriate amount of water to reach activity IV. IR stretching frequencies of CO ligands were measured in solution using CaF_2 windows, are referred to as $\nu(CO)$, and are given in cm^{-1} . Nuclear magnetic resonance (NMR) spectra were routinely recorded at room temperature in CD_2Cl_2 solutions unless otherwise stated. Chemical shifts (δ) are given in ppm, relative to internal tetramethylsilane (1H and ^{13}C), or external 85% aqueous H_3PO_4 solutions (^{31}P). Coupling constants (J) are given in hertz.

4.1. Preparation of $[MoWCp_2(\mu-H)(\mu-PCy_2)(CO)_4]$ (**1**)

Neat $PHCy_2$ (500 μL , 2.280 mmol) was added to a xylene solution (3 mL) of complexes $[Mo_2Cp_2(CO)_6]$ (0.540 g, 1.102 mmol) and $[W_2Cp_2(CO)_6]$ (0.730 g, 1.096 mmol) in a Schlenk tube equipped with a Young's valve. After closing the valve, the mixture was stirred at 453 K for 6 h to give an orange solution. The solvent was then removed under vacuum, the residue extracted with dichloromethane/petroleum ether (1/5) and the extracts chromatographed through a silica gel column (230–400 mesh) at 253 K. Elution with dichloromethane/petroleum ether (1/5) gave an orange fraction yielding, after removal of solvents, the known complex $[Mo_2Cp_2(\mu-H)(\mu-PCy_2)(CO)_4]$ as an orange solid (0.090 g, 13%). Elution with dichloromethane/petroleum ether (1/3) gave two more orange fractions analogously yielding, respectively, compound **1** (0.460 g, 29%) and the known complex $[W_2Cp_2(\mu-H)(\mu-PCy_2)(CO)_4]$ (0.080 g, 10%), as orange solids. *Data for compound 1*: Anal. Calc. for $C_{26}H_{33}MoO_4PW$: C, 43.35; H, 4.62. Found: C, 43.08; H, 4.57. 1H NMR (400.13 MHz, C_6D_6): δ 5.04, 5.02 (2s, $2 \times 5H$, Cp), 2.89 (m, 1H, Cy), 2.77 (m, 1H, Cy), 2.51, 1.78 (2m, $2 \times 2H$, Cy), 1.62 (m, 4H, Cy), 1.32 (m, 8H, Cy), 0.90, 0.15 (2m, $2 \times 2H$, Cy), -14.56 (d, $J_{HP} = 30$, $J_{HW} = 40$, 1H, $\mu-H$). $^{13}C\{^1H\}$ NMR (100.63 MHz, C_6D_6): δ 242.4 (d, $J_{CP} = 27$, MoCO), 236.4 (s, MoCO), 235.1 (d, $J_{CP} = 19$, WCO), 222.9 (s, WCO), 90.3 (s, $J_{CW} = 49$, WCp), 88.5 (s, MoCp), 41.1 [d, $J_{CP} = 20$, $2C^1(Cy)$], 32.4, 32.0 [2s, $C^2(Cy)$], 30.7 [s, $2C^2(Cy)$], 28.3, 28.1 [2d, $J_{CP} = 10$, $C^3(Cy)$], 27.4 [d, $J_{CP} = 14$, $C^3(Cy)$], 27.3 [d, $J_{CP} = 13$, $C^3(Cy)$], 27.2 [s, $2C^4(Cy)$].

4.2. Preparation of $[MoWCp_2(\mu-PCy_2)(CO)_4](BF_4)$ (**2**)

Neat $HBF_4 \cdot OEt_2$ (90 μL , 0.656 mmol) was added to a dichloromethane solution (20 mL) of compound **1** (0.350 g, 0.486 mmol), and the mixture was stirred at room temperature for 30 min to give a dark green solution which was filtered through diatomaceous earth. The solvent was then removed from the filtrate under vacuum, and the residue was washed with diethyl ether (4×8 mL) to give a dark green powder containing essentially pure compound **2**, which was used in the preparation of compound **3** without further purification. 1H NMR (400.13 MHz, CD_2Cl_2): δ 6.03, 5.86 (2s, $2 \times 5H$, Cp), 2.52–0.53 (m, 22H, Cy).

4.3. Preparation of $[MoWCp_2(\mu-I)(\mu-PCy_2)(CO)_2]$ (**3**)

Solid NaI (0.300 g, 3.336 mmol) was added to a 1,2-dichloroethane solution (15 mL) of the crude compound **2**

prepared as described in section 4.2 (ca. 0.486 mmol), and the mixture was refluxed for 90 min to give a green solution which was filtered using a canula. Removal of solvent from the filtrate gave a green solid containing essentially pure, air-sensitive compound **3**, which was used in the preparation of complex **4** without further purification. 1H NMR (300.13 MHz, C_6D_6): δ 5.01, 4.96 (2s, $2 \times 5H$, Cp), 2.40–1.07 (m, 22H, Cy).

4.4. Preparation of tetrahydrofuran suspensions of $Na[MoWCp_2(\mu-PCy_2)(\mu-CO)_2]$ (**4-Na**)

Sodium amalgam (ca. 1 mL of a 0.5% amalgam, 3 mmol) was added to a tetrahydrofuran solution (15 mL) of the crude compound **3** prepared as described in section 4.3 (ca. 0.486 mmol), and the mixture was stirred for 20 min to give an orange suspension of the very air-sensitive compound **4-Na**. This suspension was transferred with a cannula to an empty Schlenk tube, to remove the excess amalgam, and was then ready for further use.

4.5. Preparation of $[MoWCp_2(H)(\mu-PCy_2)(CO)_2]$ (**5**)

Solid $(NH_4)PF_6$ (0.120 g, 0.736 mmol) was added to a tetrahydrofuran suspension (15 mL) of compound **4-Na** (ca. 0.486 mmol) prepared as described in section 4.4, and the mixture was stirred for 5 min to give a purple solution. The solvent was then removed under vacuum, the residue extracted with dichloromethane/petroleum ether (1/5), and the extracts were filtered through diatomaceous earth. After removal of solvents from the filtrate, the residue was dissolved in dichloromethane/petroleum ether (1/5) and chromatographed on alumina at 253 K. Elution with dichloromethane/petroleum ether (1/3) gave a green band yielding, after removal of solvents, compound **5** as a purple solid (0.260 g, 80%). This compound was shown by NMR to display in solution two interconverting isomers (**B** and **T**, see text) with the equilibrium **5T**/**5B** ratio being solvent- and temperature-dependent, with 1H NMR-measured ratios of 1.8 (CD_2Cl_2 , 203 K), 2.5 (CD_2Cl_2 , 183 K) and 0.6 (toluene- d_8 , 183 K). Anal. Calc. for $C_{25}H_{35}Cl_2MoO_2PW \cdot 5 \cdot CH_2Cl_2$: C, 40.08; H, 4.71. Found: C, 39.71; H, 5.23. 1H NMR (400.13 MHz, CD_2Cl_2 , 293 K): δ 5.25, 5.18 (2s, $2 \times 5H$, Cp), 2.52–1.00 (m, 22H, Cy), -3.92 (s, br, 1H, M–H). 1H NMR (400.13 MHz, CD_2Cl_2 , 183 K): Isomer **5T**: δ 5.43, 5.31 (2s, $2 \times 5H$, Cp), -1.46 (d, $J_{HP} = 32$, $J_{HW} = 70$, W–H). Isomer **5B**: δ 5.24, 5.19 (2s, $2 \times 5H$, Cp), -6.41 (d, $J_{HP} = 3$, $J_{HW} = 118$, $\mu-H$). $^{13}C\{^1H\}$ NMR (100.63 MHz, CD_2Cl_2 , 183 K): δ 276.2 (s, WCO, **5T**), 251.0 (d, $J_{CP} = 7$, MoCO, **5T**), 246.0 (d, $J_{CP} = 10$, MoCO, **5B**), 235.8 (s, WCO, **5B**), 90.7, 90.6 (2s, Cp, **5T**), 87.9, 87.5 (2s, Cp, **5B**), 45.2, 43.3 [2d, $J_{CP} = 21$, $C^1(Cy)$, **5T**], 36.0 [d, $J_{CP} = 6$, $C^2(Cy)$, **5B**], 34.9, 33.7 [2s, $C^2(Cy)$, **5T**], 32.5, 32.3, 32.2 [3s, $C^2(Cy)$, **5B**], 31.4 [s, $2C^2(Cy)$, **5T**], 28.2–26.7 [m, $4C^3(Cy)$, **5T** and **5B**], 26.3, 26.1 [2s, $C^4(Cy)$, **5T** and **5B**]; the $C^1(Cy)$ resonances of the minor isomer **5B** could not be identified in this spectrum.

4.6. Reaction of **4-Na** with MeI

Neat MeI (40 μL , 0.643 mmol) was added to a tetrahydrofuran suspension (8 mL) of compound **4-Na** (ca. 0.120 mmol) prepared as described in section 4.4, and the mixture was stirred at room temperature for 24 h to give a brown solution. The solvent was then removed under vacuum, the residue extracted with dichloromethane/petroleum ether (1/5), and the extracts were chromatographed on alumina at 253 K. Elution with dichloromethane/petroleum ether (1/3) gave a brown fraction yielding, after removal of solvents, complex $[MoWCp_2(\mu-\kappa^1:\eta^2-CH_3)(\mu-PCy_2)(CO)_2]$ (**6**) as a brown solid (0.045 g, 55%). Elution with neat dichloromethane gave another brown fraction analogously yielding complex $[MoWCp_2(\mu-COMe)(\mu-PCy_2)(\mu-CO)]$ (**7**) as a brown solid (0.010 g, 12%). *Data for*

compound **6**: Anal. Calc. for $C_{25}H_{35}MoO_2PW$: C, 44.27; H, 5.20. Found: C, 44.37; H, 5.59. 1H NMR (400.13 MHz, CD_2Cl_2 , 233 K): δ 5.29, 5.28 (2s, $2 \times 5H$, Cp), 2.28–1.06 (m, 22H, Cy), –0.87 (d, $J_{HP} = 2$, $J_{HC} = 122$, 3H, $\mu-CH_3$). $^{13}C\{^1H\}$ NMR (100.63 MHz, CD_2Cl_2 , 233 K): δ 245.9 (d, $J_{CP} = 12$, MoCO), 241.4 (d, $J_{CP} = 8$, WCO), 88.5, 88.1 (2s, Cp), 47.0 [d, $J_{CP} = 22$, $C^1(Cy)$], 34.0, 33.9 [2d, $J_{CP} = 3$, $C^2(Cy)$], 32.7, 32.6 [2s, $C^2(Cy)$], 28.2 [d, $J_{CP} = 12$, $2C^3(Cy)$], 28.0, 27.8 [2d, $J_{CP} = 11$, $C^3(Cy)$], 26.4, 26.3 [2s, $C^4(Cy)$], –44.6 (s, $\mu-CH_3$).

4.7. Preparation of $[MoWCp_2(\mu-COMe)(\mu-PCy_2)(\mu-CO)]$ (**7**)

Neat Me_2SO_4 (30 μL , 0.317 mmol) was added to a tetrahydrofuran suspension (4 mL) of compound **4-Na** (ca. 0.060 mmol) prepared as described in section 4.4, and the mixture was stirred at room temperature for 18 h to give a brown solution. The solvent was then removed under vacuum, the residue extracted with dichloromethane/petroleum ether (1/7), and the extracts were chromatographed on alumina at 288 K. Elution with dichloromethane/petroleum ether (1/1) gave a brown fraction yielding, after removal of solvents, compound **7** as a brown solid (0.035 g, 86%). Anal. Calc. for $C_{25}H_{35}MoO_2PW$: C, 44.27; H, 5.20. Found: C, 44.68; H, 5.66. 1H NMR (400.13 MHz, C_6D_6): δ 5.82, 5.72 (2s, $2 \times 5H$, Cp), 3.33 (s, 3H, OMe), 1.92–0.38 (m, 22H, Cy). $^{13}C\{^1H\}$ NMR (100.63 MHz, C_6D_6): δ 348.3 (d, $J_{CP} = 11$, $\mu-COMe$), 298.2 (s, br, $\mu-CO$), 93.9, 93.1 (2s, Cp), 65.3 (s, OMe), 42.6, 41.7 [2d, $J_{CP} = 21$, $C^1(Cy)$], 34.4, 34.3, 33.9, 33.6 [4s, $C^2(Cy)$], 27.8–27.4 [m, $4C^3(Cy)$], 26.6, 26.4 [2s, $C^4(Cy)$].

4.8. Preparation of $[MoWCp_2(\mu-\kappa^1:\eta^2-CH_2Ph)(\mu-PCy_2)(CO)_2]$ (**8**)

Neat benzyl chloride (100 μL , 1.304 mmol) was added to a tetrahydrofuran suspension (10 mL) of compound **4-Na** (ca. 0.090 mmol) prepared as described in section 4.4, and the mixture was stirred in the dark at room temperature for 5 d to give a brown solution. The solvent was then removed under vacuum, the residue extracted with dichloromethane, and the extracts filtered through diatomaceous earth. After removal of solvent from the filtrate, the residue was now extracted with dichloromethane/petroleum ether (1/7), and the extracts were chromatographed on alumina at 288 K. Elution with dichloromethane/petroleum ether (1/5) gave a brown fraction yielding, after removal of solvents, compound **8** as a brown solid (0.050 g, 74%). The crystals used in the X-ray study were grown by the slow diffusion of layers of toluene and petroleum ether into a concentrated dichloromethane solution of the complex at 253 K. Anal. Calc. for $C_{31}H_{39}MoO_2PW$: C, 49.36; H, 5.21. Found: C, 49.09; H, 5.33. 1H NMR (300.13 MHz, CD_2Cl_2): δ 7.18 [false t, $J_{HH} = 8$, 2H, $H^3(Ph)$], 6.96 [false d, $J_{HH} = 7$, 2H, $H^2(Ph)$], 6.86 [t, $J_{HH} = 7$, 1H, $H^4(Ph)$], 5.42, 5.07 (2s, $2 \times 5H$, Cp), 2.47 (d, $J_{HH} = 15$, 1H, $\mu-CH_2Ph$), 2.37–0.98 (m, 22H, Cy), –2.02 (d, $J_{HH} = 15$, 1H, $\mu-CH_2Ph$). $^{13}C\{^1H\}$ NMR (74.48 MHz, CD_2Cl_2): δ 243.8 (d, $J_{CP} = 11$, MoCO), 240.3 (d, $J_{CP} = 8$, WCO), 155.3 [s, $C^1(Ph)$], 127.6, 127.2 [2s, $C^{2,3}(Ph)$], 122.1 [s, $C^4(Ph)$], 89.0, 87.9 (2s, Cp), 49.8 [d, $J_{CP} = 23$, $C^1(Cy)$], 47.5 [d, $J_{CP} = 22$, $C^1(Cy)$], 34.3, 34.2 [2d, $J_{CP} = 3$, $C^2(Cy)$], 33.3, 33.1 [2s, $C^2(Cy)$], 28.4 [d, $J_{CP} = 12$, $2C^3(Cy)$], 28.3 [d, $J_{CP} = 11$, $C^3(Cy)$], 28.2 [d, $J_{CP} = 10$, $C^3(Cy)$], 26.6 [s, $2C^4(Cy)$], –3.9 (s, 1H, $\mu-CH_2Ph$).

4.9. Preparation of $[MoWCp_2(\mu-CH)(\mu-PCy_2)(\mu-CO)]$ (**9**)

A toluene solution (5 mL) of compound **6** (0.030 g, 0.044 mmol) was irradiated with visible-UV light at 288 K for 30 min, with a gentle nitrogen purge, to give a brown-purple solution containing compound **9** as major product, along with significant amounts of compound **1**. The solvent was then removed under vacuum, the residue extracted with dichloromethane/petroleum ether (1/5), and the extracts were chromatographed on alumina at 253 K.

Elution with dichloromethane/petroleum ether (1/1) gave a purple fraction yielding, after removal of solvents, compound **9** as a red solid (0.020 g, 70%). Anal. Calc. for $C_{24}H_{33}MoO_2PW$: C, 44.47; H, 5.13. Found: C, 44.74; H, 5.55. 1H NMR (400.13 MHz, C_6D_6): δ 18.70 (s, $J_{HW} = 20$, 1H, $\mu-CH$), 5.84, 5.75 (2s, $2 \times 5H$, Cp), 1.83–0.63 (m, 19H, Cy), 0.48–0.33 (m, 3H, Cy). $^{13}C\{^1H\}$ NMR (100.63 MHz, C_6D_6): δ 369.4 (d, $J_{CP} = 11$, $\mu-CH$), 296.6 (d, $J_{CP} = 5$, $\mu-CO$), 94.6, 93.8 (2s, Cp), 42.6 [d, $J_{CP} = 22$, $C^1(Cy)$], 40.4 [d, $J_{CP} = 20$, $C^1(Cy)$], 34.1, 34.0, 33.7, 33.1 [4s, $C^2(Cy)$], 27.5 [d, $J_{CP} = 11$, $C^3(Cy)$], 27.4 [d, $J_{CP} = 12$, $3C^3(Cy)$], 26.4, 26.1 [2s, $C^4(Cy)$].

4.10. Photolysis of the benzyl complex **8**

A toluene solution (6 mL) of compound **8** (0.030 g, 0.040 mmol) was irradiated with visible-UV light at 288 K for 15 min, with a gentle nitrogen purge, to give a reddish brown solution containing complex $[MoWCp_2(\mu-CPh)(\mu-PCy_2)(\mu-CO)]$ (**10**) as major product, along with smaller amounts of $[MoWCp_2(\mu-PCy_2)_2(\mu-CO)]$ (**11**). The solvent was then removed under vacuum, the residue extracted with dichloromethane/petroleum ether (1/7), and the extracts were chromatographed on alumina at 288 K. Elution with dichloromethane/petroleum ether (1/3) gave a brown fraction yielding, after removal of solvents, compound **10** as a brown solid (0.018 g, 62%). Elution with neat dichloromethane gave a pink fraction yielding analogously complex **11** as a pink solid (0.006 g, 17%). Data for compound **10**: Anal. Calc. for $C_{30}H_{37}MoOPW$: C, 49.74; H, 5.15. Found: C, 49.52; H, 5.00. 1H NMR (400.13 MHz, CD_2Cl_2): δ 7.12 [false t, $J_{HH} = 8$, 2H, $H^3(Ph)$], 6.99 [t, $J_{HH} = 7$, 1H, $H^4(Ph)$], 6.57 [false d, $J_{HH} = 7$, 2H, $H^2(Ph)$], 5.94, 5.87 (2s, $2 \times 5H$, Cp), 1.98–0.93 (m, 17H, Cy), 0.68–0.48 (m, 5H, Cy). $^{13}C\{^1H\}$ NMR (100.63 MHz, CD_2Cl_2): δ 375.0 (d, $J_{CP} = 11$, $\mu-CPh$), 302.4 (d, $J_{CP} = 6$, $\mu-CO$), 166.5 [s, $C^1(Ph)$], 127.8 [s, $C^3(Ph)$], 124.1 [s, $C^4(Ph)$], 121.0 [s, $C^2(Ph)$], 96.0, 95.2 (2s, Cp), 43.6 [d, $J_{CP} = 23$, $C^1(Cy)$], 42.4 [d, $J_{CP} = 21$, $C^1(Cy)$], 34.2, 34.1, 33.6, 33.3 [4s, $C^2(Cy)$], 27.5 [d, $J_{CP} = 12$, $C^3(Cy)$], 27.5 [d, $J_{CP} = 12$, $3C^3(Cy)$], 26.4, 26.3 [2s, $C^4(Cy)$]. Data for compound **11**: 1H NMR (400.13 MHz, C_6D_6): δ 5.75, 5.64 (2s, $2 \times 5H$, Cp), 2.02–0.81 (m, 44H, Cy).

4.11. X-ray data collection, structure determination and refinements for compound **8**

X-ray intensity data were collected at ca. 140 K on an Oxford Diffraction Xcalibur Nova single crystal diffractometer, using Cu $K\alpha$ radiation. Images were collected at a 63 mm fixed crystal-detector distance using the oscillation method, with 1° oscillation and variable exposure time per image. Data collection strategy was calculated with the program CrysAlis Pro CCD [36], and data reduction and cell refinement was performed with the program CrysAlis Pro RED [36]. An empirical absorption correction was applied using the SCALE3 ABSPACK algorithm as implemented in the program CrysAlis Pro RED. Twinning was present in the crystal, but the twin law could not be found. Using the program suite WINGX [37], the structure was solved by Patterson interpretation and phase expansion using SHELXL2016 [38], and refined with full-matrix least squares on F^2 using SHELXL2016 to give the residuals shown in Table 4. All non-hydrogen atoms were refined anisotropically except for a few atoms which had to be refined anisotropically in combination with the instructions DELU and SIMU. A slight disorder was present in one Cp ligand, which could not be modelled. All hydrogen atoms were geometrically placed and refined using a riding model except for H(4), which was located on the Fourier maps and refined isotropically; in the latter case, however, a restraint on the C(3)–H(4) and Mo(1)–H(4) bond lengths was necessary to obtain a satisfactory refinement of its position.

Table 4
Crystal data for compound **8**.

Mol formula	C ₃₁ H ₃₉ MoO ₂ PW
Mol weight	754.38
Cryst syst	Monoclinic
Space group	<i>P</i> 2 ₁ / <i>c</i>
Radiation (λ, Å)	1.54184
<i>a</i> (Å)	9.7948(6)
<i>b</i> (Å)	29.0742(15)
<i>c</i> (Å)	10.2085(7)
α (°)	90
β (°)	108.666(7)
γ (°)	90
<i>V</i> (Å ³)	2754.2(3)
<i>Z</i>	4
Calcd density (g cm ⁻³)	1.819
Absorp coeff. (mm ⁻¹)	12.083
Temperature (K)	140.0(1)
θ range (°)	3.04 to 69.47
index ranges (<i>h</i> , <i>k</i> , <i>l</i>)	–11, 7; –31, 35 –11, 12
No. of reflns collected	10,779
No. of indep reflns (<i>R</i> _{int})	4636 (0.0839)
Reflns with <i>I</i> > 2σ(<i>I</i>)	3953
<i>R</i> indexes [data with <i>I</i> > 2σ(<i>I</i>)] ^a	<i>R</i> ₁ = 0.0901, <i>wR</i> ₂ = 0.2481 ^b
<i>R</i> indexes (all data) ^b	<i>R</i> ₁ = 0.1064, <i>wR</i> ₂ = 0.2743 ^b
GOF	1.104
No. of restraints/params	47/329
Δρ(max., min.), eÅ ⁻³	3.447/–3.521
CCDC deposition no	1901013

$$^a R_1 = \frac{\sum ||F_o| - |F_c||}{\sum |F_o|}, \quad wR_2 = \frac{[\sum w(|F_o|^2 - |F_c|^2)^2 / \sum w|F_o|^2]^{1/2}}{[\sigma^2(F_o^2) + (aP)^2 + bP]} \quad \text{where } P = (F_o^2 + 2F_c^2)/3, \quad w = 1/$$

$$^b a = 0.1535, b = 87.7871.$$

4.12. DFT calculations

All DFT calculations were carried out using the GAUSSIAN03 package [39], in which the hybrid method B3LYP was used with the Becke three-parameter exchange functional [40], and the Lee-Yang-Parr correlation functional [41]. A pruned numerical integration grid (99,590) was used for all the calculations via the keyword Int = Ultrafine. Effective core potentials and their associated double-ζ LANL2DZ basis set were used for Mo and W atoms [42]. The light elements (P, O, C and H) were described with the 6-31G* basis [43]. Geometry optimizations were performed under no symmetry restrictions, using initial coordinates derived from the X-ray data of closely related compounds, and frequency analyses were performed for all the stationary points to ensure that a minimum structure with no imaginary frequencies was achieved. The effect of dichloromethane on the stability of isomers **5B** and **5T** in solution was modelled through the polarized-continuum-model (PCM) of Tomasi and co-workers [44], using the gas-phase optimized structures. The effect of dispersion forces on the relative stability of these isomers was estimated by using the empirical dispersion corrections developed by Grimme [45].

Declaration of interests

None.

Acknowledgment

This work is dedicated to the memory of the late Prof. Pascual Royo, in recognition for his outstanding contribution to Organometallic Chemistry in Spain. This research was funded by the MINECO of Spain and FEDER (Project CTQ2015-63726-P, and a grant to E.H.), and the Consejería de Educación of Asturias (Project

GRUPIN14-011). We also thank the X-Ray unit of Universidad de Oviedo, Spain, for acquisition of diffraction data, and the CMC unit of Universidad de Oviedo for access to computing facilities.

Appendix A. Supplementary Data

An XYZ file containing the Cartesian coordinates for all computed species. CCDC 1901013 contains the supplementary crystallographic data for compound **8**; these data can be obtained free of charge from The Cambridge Crystallographic Data Centre via www.ccdc.cam.ac.uk/data_request/cif.

References

- (a) F.A. Cotton, G. Wilkinson, *Advanced Inorganic Chemistry*, fifth ed., Wiley, New York, 1988 (Chapter 22);
(b) J.E. Ellis, *Adv. Organomet. Chem.* 31 (1990) 151;
(c) J.E. Ellis, *Inorg. Chem.* 45 (2006) 3167 (and references therein).
- (a) C. Chi, S. Pan, L. Meng, M. Luo, L. Zhao, M. Zhou, G. Frenking, *Angew. Chem. Int. Ed.* 58 (2019) 1732;
(b) L. Jin, T. Yang, K. Xin, G. Wang, X. Jin, M. Zhou, G. Frenking, *Angew. Chem. Int. Ed.* 57 (2018) 6236.
- (a) X.Y. Liu, V. Riera, M.A. Ruiz, M. Lanfranchi, A. Tiripicchio, *Organometallics* 22 (2003) 4500 (and references therein).
- D. Seyferth, K.S. Brewer, T.G. Wood, M. Cowie, R.W. Hilt, *Organometallics* 11 (1992) 2570.
- (a) M.E. García, S. Melón, A. Ramos, M.A. Ruiz, *Dalton Trans.* (2009) 8171;
(b) M.E. García, S. Melón, A. Ramos, V. Riera, M.A. Ruiz, D. Belletti, C. Graiff, A. Tiripicchio, *Organometallics* 22 (2003) 1983.
- M.A. Alvarez, M. Casado-Ruano, M.E. García, D. García-Vivó, M.A. Ruiz, *Inorg. Chem.* 56 (2017) 11336.
- (a) M.A. Alvarez, M.E. García, D. García-Vivó, M.A. Ruiz, M.F. Vega, *Organometallics* 34 (2015) 870;
(b) M.A. Alvarez, M.E. García, D. García-Vivó, M.A. Ruiz, M.F. Vega, *Organometallics* 29 (2010) 512.
- D. García-Vivó, A. Ramos, M.A. Ruiz, *Coord. Chem. Rev.* 257 (2013) 2143.
- M.A. Alvarez, M.E. García, D. García-Vivó, M.A. Ruiz, M.F. Vega, *Dalton Trans.* 43 (2014) 16044.
- In this paper we have adopted a “half-electron” counting convention for complexes displaying bridging hydrides, so hydride isomers **B** and **T** are both regarded as having a M≡M bond, thus emphasizing their highly and similarly unsaturated nature. Other authors, however, recommend the adoption of a “half-arrow” convention for all hydride-bridged complexes (see M.L.H. Green, C. Parkin, *Struct. Bond* 117 (2017) [79], and references therein). For a recent discussion on both views on hydride-bridged complexes, see reference 11.
- (a) M.L.H. Green, *Dalton Trans.* 47 (2018) 6628;
(b) D. García-Vivó, M.A. Ruiz, *Dalton Trans.* 47 (2018) 6630.
- (a) R.J. Eisenhart, L.J. Clouston, C.C. Lu, *Acc. Chem. Res.* 48 (2015) 2885;
(b) J.P. Krogman, C.M. Thomas, *Chem. Commun.* 540 (2014) 511;
(c) C.M. Thomas, *Comments Inorg. Chem.* 32 (2011) 14;
(d) J.P. Collman, R. Boulatov, *Angew. Chem. Int. Ed.* 41 (2002) 3948.
- V. Rittler, M.J. Chetcuti, *Chem. Rev.* 107 (2007) [797].
- (a) S. Clapham, P. Braunstein, N.M. Boag, R. Welter, M.J. Chetcuti, *Organometallics* 27 (2008) 1758;
(b) M. Oishi, M. Oshima, H. Suzuki, *Inorg. Chem.* 53 (2014) 6634;
(c) M. Oishi, M. Kino, M. Saso, M. Oshima, H. Suzuki, *Organometallics* 31 (2012) 4658;
(d) H. Kameo, Y. Nakajima, H. Suzuki, *Angew. Chem. Int. Ed.* 47 (2008) 10159.
- M.E. García, V. Riera, M.A. Ruiz, M.T. Rueda, D. Sáez, *Organometallics* 21 (2002) 5515.
- C.M. Alvarez, M.A. Alvarez, D. García-Vivó, M.E. García, M.A. Ruiz, D. Sáez, L.R. Falvello, T. Soler, P. Herson, *Dalton Trans.* (2004) 4168.
- (a) H.-J. Haupt, A. Merla, U. Flörke, Z. Anorg. Allg. Chem. 620 (1994) 999;
(b) H.-J. Haupt, U. Flörke, G. Disse, C. Heinekamp, *Chem. Ber.* 124 (1991) 2191.
- C.M. Alvarez, M.A. Alvarez, M. Alonso, M.E. García, M.T. Rueda, M.A. Ruiz, P. Herson, *Inorg. Chem.* 45 (2006) 9593.
- A general trend established for ²J_{XY} in complexes of the type [MCpXYL₂] is that |J_{cis}| > |J_{trans}|. See, for instance, reference 20 B. Wrackmeyer, H.G. Alt, H.E. Maisel, *J. Organomet. Chem.* 399 (1990) 125.
- C.J. Jameson, in: J.G. Verkade, L.D. Quin (Eds.), *Phosphorus-31 NMR Spectroscopy in Stereochemical Analysis*, VCH, New York, 1987 (Chapter 6).
- C.M. Alvarez, M.E. García, M.T. Rueda, M.A. Ruiz, D. Sáez, N.G. Connelly, *Organometallics* 24 (2005) 650.
- P.S. Braterman, *Metal Carbonyl Spectra*, Academic Press, London, U.K., 1975.
- C.M. Alvarez, M.A. Alvarez, M.E. García, A. Ramos, M.A. Ruiz, M. Lanfranchi, A. Tiripicchio, *Organometallics* 24 (2005) [7].
- (a) C.J. Cramer, *Essentials of Computational Chemistry*, second ed., Wiley, Chichester, UK, 2004;
(b) W. Koch, M.C. Holthausen, *A Chemist's Guide to Density Functional Theory*, second ed., Wiley-VCH, Weinheim, 2002.

- (25) (a) R.M. Bullock, *Comments Inorg. Chem.* 12 (1991) 1;
(b) J.A. Martinho Simoes, J.L. Beauchamp, *Chem. Rev.* 90 (1990) 629;
(c) R.G. Pearson, *Chem. Rev.* 85 (1985) 41.
- [26] R.H. Crabtree, M. Lavin, *Inorg. Chem.* 25 (1986) 805.
- [27] V.A. Levina, O.A. Filippov, E.I. Gutsul, N.V. Belkova, L.M. Epstein, A. Lledós, E.S. Shubina, *J. Am. Chem. Soc.* 132 (2010) 11234 (and references therein).
- [28] M.A. Alvarez, M.E. García, D. García-Vivó, M.E. Martínez, M.A. Ruiz, *Organometallics* 30 (2011) 2189.
- [29] M.E. García, A. Ramos, M.A. Ruiz, M. Lanfranchi, L. Marchiò, *Organometallics* 26 (2007) 6197.
- [30] The η^2 -coordination of the Alkyl Ligand Likely Will Be Stronger Also at the W (Vs. Mo) Site; However, since the Strength of the η^2 -coordination (Below Ca. 100 kJ/mol) Is Much Lower than the Strength of the κ^1 -coordination (Around 200 kJ/mol), the Overall Thermodynamic Balance Will Be in Favour of κ^1 -coordination to the W Atom.
- [31] M.A. Alvarez, M.E. García, D. García-Vivó, M.E. Martínez, A. Ramos, M.A. Ruiz, *Organometallics* 27 (2008) 1973.
- [32] T. Adatia, M. McPartlin, M.J. Mays, M.J. Morris, P.R. Raithby, *J. Chem. Soc., Dalton Trans.* (1989) 1555.
- [33] M.E. García, D. García-Vivó, M.A. Ruiz, S. Alvarez, G. Aullón, *Organometallics* 26 (2007) 4930.
- [34] W.L.F. Armarego, C.C.C. Chai, *Purification of Laboratory Chemicals*, seventh ed., Butterworth-Heinemann, Oxford, U. K., 2012.
- [35] R. Birdwhistell, P. Hackett, A.R. Manning, *J. Organomet. Chem.* 157 (1978) 239.
- [36] *CrysAlis Pro*, Oxford Diffraction Limited, Ltd., Oxford, U. K., 2006.
- [37] L.J. Farrugia, *J. Appl. Crystallogr.* 32 (1999) [837].
- [38] (a) G.M. Sheldrick, *Acta Crystallogr. A* 64 (2008) 112;
(b) G.M. Sheldrick, *Acta Crystallogr. C* 71 (2015) 5.
- [39] M.J. Frisch, G.W. Trucks, H.B. Schlegel, G.E. Scuseria, M.A. Robb, J.R. Cheeseman, J.A. Montgomery Jr., T. Vreven, K.N. Kudin, J.C. Burant, J.M. Millam, S.S. Iyengar, J. Tomasi, V. Barone, B. Mennucci, M. Cossi, G. Scalmani, N. Rega, G.A. Petersson, H. Nakatsuji, M. Hada, M. Ehara, K. Toyota, R. Fukuda, J. Hasegawa, M. Ishida, T. Nakajima, Y. Honda, O. Kitao, H. Nakai, M. Klene, X. Li, J.E. Knox, H.P. Hratchian, J.B. Cross, V. Bakken, C. Adamo, J. Jaramillo, R. Gomperts, R.E. Stratmann, O. Yazyev, A.J. Austin, R. Cammi, C. Pomelli, J.W. Ochterski, P.Y. Ayala, K. Morokuma, G.A. Voth, P. Salvador, J.J. Dannenberg, V.G. Zakrzewski, S. Dapprich, A.D. Daniels, M.C. Strain, O. Farkas, D.K. Malick, A.D. Rabuck, K. Raghavachari, J.B. Foresman, J.V. Ortiz, Q. Cui, A.G. Baboul, S. Clifford, J. Cioslowski, B.B. Stefanov, G. Liu, A. Liashenko, P. Piskorz, I. Komaromi, R.L. Martin, D.J. Fox, T. Keith, M.A. Al-Laham, C.Y. Peng, A. Nanayakkara, M. Challacombe, P.M.W. Gill, B. Johnson, W. Chen, M.W. Wong, C. Gonzalez, J.A. Pople, *Gaussian 03, Revision B.02*, Gaussian, Inc., Wallingford, CT, 2004.
- [40] A.D. Becke, *J. Chem. Phys.* 98 (1993) 5648.
- [41] C. Lee, W. Yang, R.G. Parr, *Phys. Rev. B* 37 (1988) 785.
- [42] P.J. Hay, W.R. Wadt, *J. Chem. Phys.* 82 (1985) [299].
- [43] (a) P.C. Hariharan, J.A. Pople, *Theor. Chim. Acta* 28 (1973) 213;
(b) G.A. Petersson, M.A. Al-Laham, *J. Chem. Phys.* 94 (1991) 6081;
(c) G.A. Petersson, A. Bennett, T.G. Tensfeldt, M.A. Al-Laham, W.A. Shirley, J. Mantzaris, *J. Chem. Phys.* 89 (1988) 2193.
- [44] M. Cossi, V. Barone, R. Cammi, J. Tomasi, *Chem. Phys. Lett.* 255 (1996) 327 (and references therein).
- [45] S. Grimme, *J. Comput. Chem.* 27 (2006) 1787.